Biochemical and Biophysical Research Communications 459 (2015) 107–112

Contents lists available at ScienceDirect

Biochemical and Biophysical Research Communications

journal homepage: www.elsevier.com/locate/ybbrc

Toxoplasma gondii: Biochemical and biophysical characterization of recombinant soluble dense granule proteins GRA2 and GRA6

Amina Bittame [a, b], Grégory Effantin [c, d, e, f], Graciane Pètre [a, b], Pauline Ruffiot [a, b, 1], Laetitia Travier [a, b, 2], Guy Schoehn [c, d, e, f], Winfried Weissenhorn [c, d, e, f], Marie-France Cesbron-Delauw [a, b], Jean Gagnon [a, b, 3], Corinne Mercier [a, b, *, 3]

[a] CNRS, UMR 5163, 38042 Grenoble, France
[b] Université Grenoble Alpes, 38042 Grenoble, France
[c] Université Grenoble Alpes, Institut de Biologie Structurale (IBS), 38044 Grenoble, France
[d] CNRS, IBS, 38044 Grenoble, France
[e] CEA, IBS, 38044 Grenoble, France
[f] Unit for Virus Host-Cell Interactions (UVHCI), UMI 3265 (UJF-EMBL-CNRS), 38027 Grenoble, France

ARTICLE INFO

Article history:
Received 9 February 2015
Available online 21 February 2015

Keywords:
Amphipathic alpha-helices
Dense granule proteins (GRA)
Toxoplasma gondii
Circular dichroism
Dynamic light scattering
Transmission electron microscopy

ABSTRACT

The most prominent structural feature of the parasitophorous vacuole (PV) in which the intracellular parasite *Toxoplasma gondii* proliferates is a membranous nanotubular network (MNN), which interconnects the parasites and the PV membrane. The MNN function remains unclear. The GRA2 and GRA6 proteins secreted from the parasite dense granules into the PV have been implicated in the MNN biogenesis. Amphipathic alpha-helices (AAHs) predicted in GRA2 and an alpha-helical hydrophobic domain predicted in GRA6 have been proposed to be responsible for their membrane association, thereby potentially molding the MMN in its structure. Here we report an analysis of the recombinant proteins (expressed in detergent-free conditions) by circular dichroism, which showed that full length GRA2 displays an alpha-helical secondary structure while recombinant GRA6 and GRA2 truncated of its AAHs are mainly random coiled. Dynamic light scattering and transmission electron microscopy showed that recombinant GRA6 and truncated GRA2 constitute a homogenous population of small particles (6–8 nm in diameter) while recombinant GRA2 corresponds to 2 populations of particles (~8–15 nm and up to 40 nm in diameter, respectively). The unusual properties of GRA2 due to its AAHs are discussed.

1. Introduction

Toxoplasma gondii is the intracellular protozoan parasite responsible for toxoplasmosis, a widespread anthropozoonosis that affects up to one half of the human population and is responsible for severe fetal disabilities or lethal encephalitis in immunocompromised patients. Like the other parasites of the Apicomplexa phylum, such as *Plasmodium spp*, *T. gondii* multiplies within a parasitophorous vacuole (PV) that provides a safe and metabolically active intracellular compartment. The PV is formed upon active invasion of the host cell, from the cellular plasma membrane and from parasite secretory products coordinately released from parasite's secretory organelles, namely the micronemes, the rhoptries and the dense granules [1–3].

The most important structural feature within the Toxoplasma PV is a membranous nanotubular network (MNN), which interconnects the parasites and links them to the PV membrane. The further function of the MNN remains unclear: it might be involved in the acquisition of nutrients from the host cell and/or the export of degradation products from the PV into the host cell [4,5]; it could maintain the dividing parasites in an ordered arrangement within the PV to optimize their synchronous division [6,7]; it could be involved in the transport of secreted protein complexes en route to

Abbreviations: aa, amino acid; AAH, amphipatic α-helix; mAb, monoclonal antibody; MNN, membranous nanotubular network; PV, parasitophorous vacuole.

* Corresponding author. Université Grenoble Alpes, 38042 Grenoble, France. Fax: +33 (0) 4 76 63 74 97.
E-mail address: corinne.mercier@ujf-grenoble.fr (C. Mercier).
[1] Equal Opportunities Office, Swiss Federal Institute of Technology of Lausanne, 1015, Lausanne, Switzerland.
[2] Pasteur Institute, Biology of Infection Unit, INSERM U1117, Paris, France.
[3] Equal contributions.

http://dx.doi.org/10.1016/j.bbrc.2015.02.078
0006-291X/

the PV membrane [8]. Furthermore, the MNN was correlated to the parasite's virulence [9].

The proteins GRA2 and GRA6, secreted from the dense granules into the PV, are currently considered as important effector candidates of MNN biogenesis. GRA2 is a 28 kDa protein (185 amino acids (a.a.)), which is predicted, depending on the program that is used, to contain two or three central amphipathic alpha-helices (AAHs) flanked by two hydrophilic regions [7]. Transmission electron microscopy (TEM) analysis of the PV of a parasite strain from which the single *gra2* gene had been deleted showed complete disruption of the MNN [7,10], demonstrating indirectly that GRA2 is a crucial effector of MNN formation. By complementation of this mutant with truncated GRA2 proteins, both the N-terminal hydrophilic domain and the AAHs were shown to be necessary to induce the formation of the MNN [7]. Interestingly, deletion of the unique *gra6* gene also resulted in parasite PVs devoid of their MNN, which was replaced by small vesicles within the vacuolar space [10]. These results indicate that GRA6 also contributes significantly to the MNN formation, maybe by stabilizing the membranous tubules induced by GRA2.

Despite these clues about the potential function of both GRA2 and GRA6 in generating the proteo-membranous tubes that constitute the MNN, nothing is known regarding the biochemical and biophysical properties of these proteins. In this study, we report main properties of recombinant GRA2 (rGRA2) and GRA6 (rGRA6) expressed in detergent-free conditions.

2. Material and methods

2.1. Antibodies

The recombinant proteins were detected using the mouse monoclonal antibody (mAb) TG 17-179 which recognizes the 8 C-terminal a.a. of GRA2 [11,12] (Biotem, France), a rabbit serum directed against the full length denatured recombinant GRA6 (gift from L.D. Sibley) [13], or the mAb Ab-1 anti-Hisx6 (Oncogene; gift from M.A. Hakimi).

2.2. Purification of recombinant proteins

We set up conditions of detergent-free purification from *Escherichia coli*, of the recombinant soluble proteins rGRA2 (theoretical molecular weight (tMW): 27.29 kDa) [14], rGRA6 (tMW: 28.38 kDa) and rGRA2 (NT-CT) (tMW: 18.41 kDa), using the pUET1 expression plasmid vector [15] (Supplementary Fig. 1). rGRA2 (NT-CT) is a truncated rGRA2, from which the 3 AAHs have been deleted. pUET1 allows fusion of the recombinant proteins with a N-terminal S tag derived from a pancreatic ribonuclease (solubilizing peptide) and with two flanking Hisx6 tags (Supplementary Fig. 1).

The pUET-GRA2 (21-185) (RH) [14], pUET-GRA2 (NT-CT) (RH) and pUET-GRA6 (43-230) (RH) constructs (see the Supplementary Data for details) were transformed into C41 (DE3) *E. coli* bacteria (Lucigen Corporation, Middleton, WI). Expression was induced for 4 h, at 33 °C, in Terrific Broth supplemented with 50 μg/mL Ampicillin and 1 mM Iso-Propyl-Thio-Galactoside. Following centrifugation, the bacteria pellets were dispersed in 20 mM 3-(N-morpholino)propanesulfonic acid (MOPS) supplemented with a cocktail of protease inhibitors without EDTA (Roche) and bacteria were lyzed mechanically using a French Press (Bioritech). Following a 20 min centrifugation at 100,000 × g, 4 °C, each supernatant was incubated for 2 h, at 4 °C, under gentle agitation, with Ni^{2+} - NTA Agarose (Qiagen) pre-equilibrated in 20 mM MOPS pH 7. 5 – protease inhibitors. After a first wash with 20 mL of 20 mM MOPS pH 7.5–5 mM imidazole and a second wash with 20 mL of 20 mM MOPS pH 7.5–60 mM Imidazole, the bound proteins were eluted with 500 mM imidazole, pH 7. Imidazole was eliminated by size exclusion chromatography on a Sephadex G-25M (GE Healthcare) equilibrated with 20 mL of 20 mM MOPS pH 7.5. The eluted fractions were concentrated using a 10 kDa Centriprep (Millipore). Protein concentrations were determined using a Bio-Rad Protein Assay Kit (Bio-Rad). Aliquoted proteins were frozen at −80 °C until being used. Upon thawing, the recombinant proteins were centrifuged for 15 min, at 4 °C and at 10,000 × g to eliminate potential aggregates. The content in soluble proteins present in the supernatants was determined prior any further experiment.

Colloid Coomassie G-250 staining after 13% SDS-PAGE (Fig. 1A) revealed major bands at the MW of 34 kDa (rGRA2), 27 kDa (rGRA2 (NT-CT)) and 43 kDa (rGRA6), respectively. Bands observed at higher apparent MW could correspond to SDS-resistant multimeric forms of rGRA2 and rGRA6, and bands at lower apparent MW could be degradation products.

Proteins separated on 13% SDS-PAGE were transferred to nitrocellulose. The membranes were blocked for 1 h with saturation solution (PBS containing 5% powder milk, 5% normal goat serum, 0.05% Tween-20 and 0.05% Triton-X114), incubated for 1 h with the appropriate primary antibody diluted in saturation solution. After

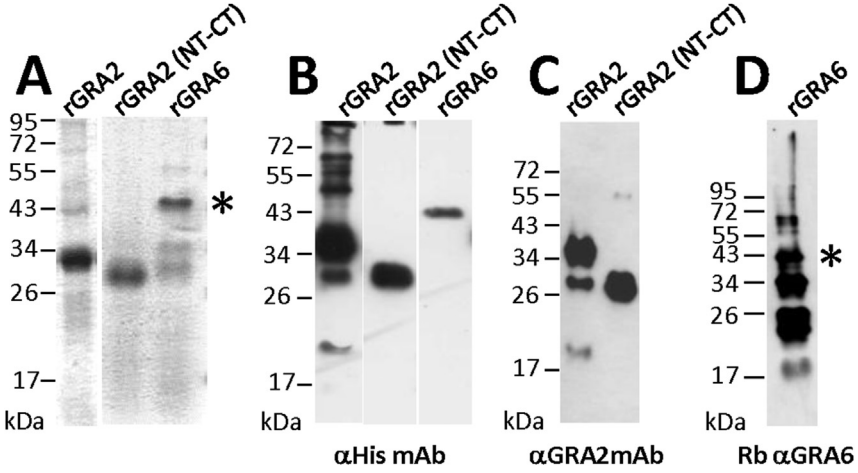

Fig. 1. SDS-PAGE analysis of the recombinant proteins rGRA2, rGRA2 (NT-CT), and rGRA6, as detected by colloid Coomassie G-250 (A) or immuno-revealed using anti-HisX6 mAb (B; α-His mAb); anti-GRA2 mAb (C; α-GRA2 mAb), or rabbit serum anti-GRA6 (D; Rb α-GRA6). Two μg of each recombinant protein were loaded per lane. The stars indicate the full length rGRA6. Anti-GRA2 mAb: 1/20,000; anti-HisX6 mAb: 1/1000; rabbit serum anti-GRA6: 1/10,000; secondary antibodies: 1/20,000.

incubation with peroxidase-conjugated goat secondary antibodies (Jackson Immunoresearch Laboratories), proteins were visualized by chemiluminescence using the Supersignal ECL system (Pierce Chemical). On immunoblots, each recombinant protein was efficiently recognized by the anti-Hisx6 mAb (Fig. 1B) as well as by antibodies specific of each GRA protein, i.e. the mAb TG17.179, which recognizes the 8 C-terminal amino acids of GRA2 [12] (Fig. 1C) and the rabbit serum raised against a denatured rGRA6 [13] (Fig. 1D).

2.3. Prediction of protein secondary structure

The secondary structure of the recombinant proteins was predicted using the GOR secondary structure prediction method (http://npsa-pbil.ibcp.fr/cgi-bin/npsa_automat.pl?page=npsa_gor4.html) [16] available at the Expert Protein Analysis System proteomics server (ExPASy server) (http://kr.expasy.org/). The GRA2 AAHs were predicted using the Heliquest program (http://heliquest.ipmc.cnrs.fr/).

2.4. Circular dichroism (CD)

CD spectra were recorded at 20 °C, from soluble recombinant proteins diluted at 15 μM in [20 mM MOPS, pH 7–500 mM NaCl - protease inhibitors] (rGRA2 and rGRA2 (NT-CT)) or in [0.02 M $NaPO_4$ pH 7.4 – protease inhibitors] (rGRA6) using a spectropolarimeter J – 810 (Jasco) coupled to a temperature-regulating device and 0.1 cm-optical path cuvettes. The CD spectra were recorded between 250 and 200 nm. The presented spectra are the mean of 4 independent accumulations from which the buffer spectrum was subtracted.

2.5. Dynamic light scattering (DLS)

Fifteen μg of each recombinant protein diluted in 50 μL of [10 mM HEPES pH 7.4–150 mM NaCl] were analyzed at 25 °C, on a « Zetasizer dedicated to proteins » (Malvern Instruments).

2.6. Transmission electron microscopy (TEM)

2-3 μL of each recombinant protein at 2 mg/mL (rGRA2), 0.1 mg/mL (rGRA2 (NT-CT)) or 0.05 mg/mL (rGRA6) in 10 mM HESPES pH 7.4–150 mM NaCl were adsorbed on the clean side of a carbon film which had been pre-evaporated on a mica sheet. The carbon film was detached from the mica by floating it in a well containing the negative stain solution: all samples were contrasted with 2% (w/v) uranyl acetate (pH 4.5) except purified rGRA6, which was contrasted with 2% sodium silicotungstate (pH 7.0). The carbon film was picked up onto a 400 mesh copper grid and air dried before observation with a JEOL 1200 EX II operating at 100 kV. Images were recorded on a 2.7 k by 2.7 k Gatan ORIUS CCD camera at the nominal magnifications of x10,000 or x40,000.

3. Results

3.1. rGRA2 folds in α-helical structure

The CD spectrum of rGRA2 displayed two minima, at 208 and 223 nm, respectively. Both these wave length minima are characteristic of a protein mainly folded in α-helical structure (Fig. 2). In agreement with the truncation of its AAHs, the spectrum of rGRA2 (NT-CT) was that of a protein arranged mainly in random coil (Fig. 2). Interestingly, the spectrum of rGRA6 showed a very small amount of α-helical structure (see the minimum at 224 nm) (Fig. 2).

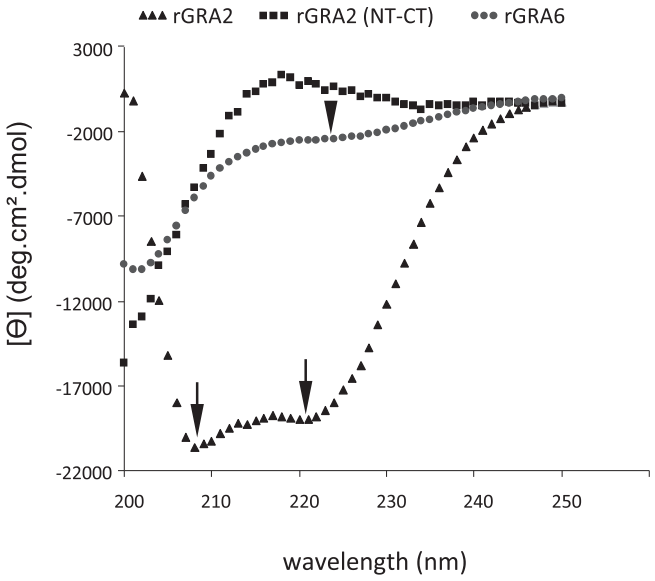

Fig. 2. Circular dichroism spectra of rGRA2 (triangles), rGRA2 (NT-CT) (squares) and rGRA6 (dots) registered between 200 and 250 nm. The arrows indicate both the 208 and 223 nm minima of the rGRA2 spectrum; the arrowhead, the 224 nm minimum of the rGRA6 spectrum.

3.2. rGRA6 and rGRA2 (NT-CT) form a homogenous population of particles while rGRA2 forms 2 populations of particles

While both rGRA2 (NT-CT) and rGRA6 appeared as homogenous populations of small particles (8 nm and 7 nm in diameter, respectively) by dynamic light scattering, 2 populations of particles were observed in the soluble rGRA2: 56% of rGRA2 was included in particles of 17.7 nm in diameter while 44% of the protein was comprised in particles of 66 nm in diameter (Fig. 3A). Although the diameter of these rGRA2 particles could not be confirmed when using a DLS Wyatt technology apparatus because of the low amplitude of the refraction index peaks, calibration of the Sephacryl-500 column coupled to the detector with soluble proteins of defined MW showed that the largest particles of rGRA2 would be > 500 kDa (data not shown).

In order to gain more information into the oligomeric forms of both rGRA2 and rGRA6, we analyzed them by negatively stained TEM. For rGRA2, we observed a continuum of structures ranging from 8 to more than 100 nm in diameter (maximum dimensions). In conjunction with the DLS results, we interpreted the smallest rGRA2 particles (i.e. around ~10 nm in diameter) as soluble small oligomers (Fig. 3B, left panel, black circles). While we cannot exclude the possibility that the very large donuts-like objects (up to 100 nm in diameter) might be vesicles/membrane pieces co-purifying with the protein, the intermediate sized structures ranging from ~15 to 40 nm in diameter (maximum dimensions) likely represent the >500 kDa multimeric forms of rGRA2, either soluble or membrane-bound (Fig. 3B, left panel, white arrows). When rGRA6 was observed by negatively stained TEM, it revealed an homogenous population of particles: their external diameter was ~6–8 nm in maximal dimension (Fig. 3B, right panel, white circles).

Together, these results led to conclude that 1) soluble rGRA2 forms a variety of oligomeric structures, the biggest ones reaching >500 kDa and forming particles up to 40 nm in diameter and 2) rGRA6 was purified as an homogeneous population of particles (~6–8 nm in diameter) that contained small oligomeric forms of the protein.

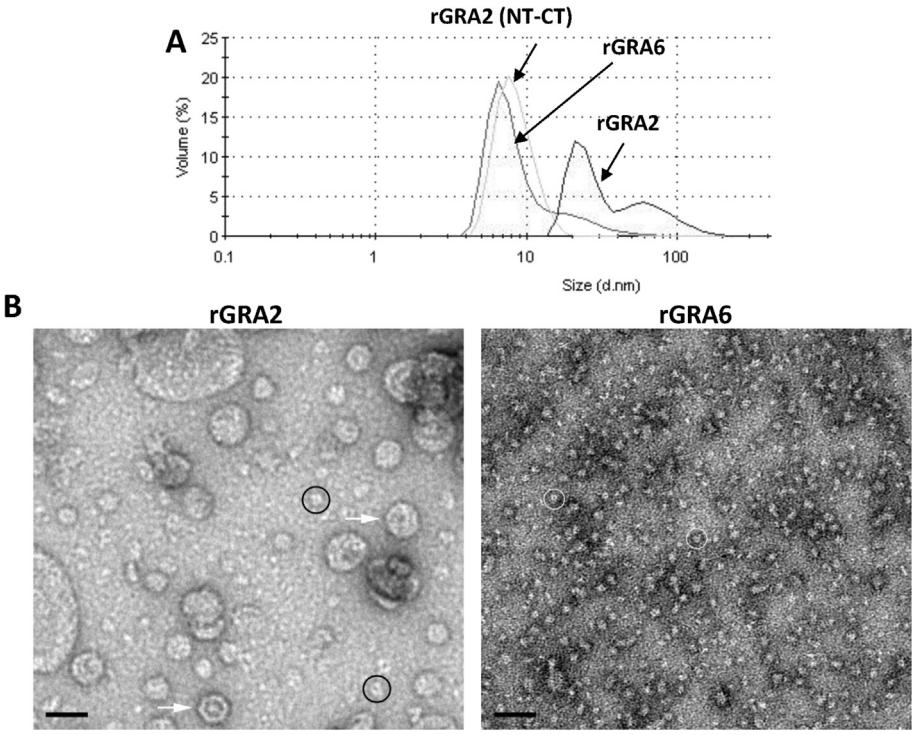

Fig. 3. Analysis of the homogeneity of soluble recombinant GRA proteins. (A) Dynamic light scattering analysis of soluble rGRA2, rGRA2 (NT-CT) and rGRA6 using a Zetasizer. (B) Transmission electron microscopy analysis of rGRA2 (left) and rGRA6 (right), White arrows and black circles indicate the rGRA2 large and small oligomers, respectively while white circles point out rGRA6 particles. Bars: 20 nm.

4. Discussion

Purification of recombinant membrane-associated proteins is always tricky and that of both rGRA2 and rGRA6 was not less difficult. After having tested several plasmid vectors, we achieved the purification of both these proteins from *E. coli*, using the pUET1 expression vector [15], which allowed solubilization of the recombinant proteins by N-terminal fusion with a peptide derived from a pancreatic ribonuclease. This 12 a.a. peptide, the Hisx6 tags and the linkers which are fused to the expressed proteins (Supplementary Fig. 1), are rather short as compared to the length of the GRA sequences. Nevertheless, addition of this ribonuclease peptide, which is predicted to adopt an α-helical structure, slightly increased the percentage of predicted α-helix in both rGRA2 (33.90%) and rGRA6 (26.50%), compared to native GRA2 (30.25%) and GRA6 (22.46%) (Table 1). Interestingly, rGRA2 displayed a CD signal characteristic of α-helical pattern (Fig. 2), despite only 33.90% of its sequence being predicted in α-helix (Table 1). This could indicate that, due to the presence of its AAHs, GRA2 is likely structured in α-helix as soon as secreted into the vacuolar space, *i.e.* before its association with the MNN. Removal of the AAHs (rGRA2 (NT-CT), Supplementary Fig. 1) led to a protein mainly in random coil (Fig. 2), thus confirming the intrinsic α-helical structure of GRA2. On the opposite, the rGRA6 CD spectrum displayed a very weak signal of α-hydrophobicity (Fig. 2), which likely underscores the 26.50% of predicted α-helical structure (Table 1). According to the Garnier secondary structure prediction program [16], most of this α-helical pattern corresponds to the 21 a.a. long potential transmembrane domain (Supplementary Fig. 1). Together, this suggests that the GRA6 hydrophobic α-helical transmembrane domain is not exposed at the surface of the protein when it is placed in an aqueous environment. Adding the fact that the N-terminal hydrophilic domain of GRA6 1) is crucial for the proper targeting of the protein to the MNN and 2) displays affinity for negatively charged phospholipids [17], one might suggest that GRA6 would 1) be secreted into the PV and travel in the vacuolar space as a soluble form, with its hydrophobic α-helical domain buried within the protein until the exposed N-terminal hydrophilic domain reaches the MNN; 2) the N-terminal domain would then attach the protein to negatively charged phospholipids of the MNN, 3) this step triggering a protein conformational change that would expose the hydrophobic transmembrane domain for interaction with the phospholipids. Defining the topology of GRA6 in the MNN will help refining this model of membrane association.

Despite the use of protease inhibitors along the purification steps, several degradation products were observed for rGRA6, with two major polypeptides migrating at 36 and 26 kDa, respectively (Fig. 1). The fact that rGRA6 was only partially folded with an α-helical pattern, the rest of the protein remaining in random coil (Fig. 2), could explain this particular sensitivity to proteases. Given that, on immunoblot, the rGRA6 degradation products were only revealed by antibodies specific to GRA6 and not by those specific to

Table 1
Comparison of the secondary structures, predicted by the GOR prediction method version IV [16] for rGRA2, rGRA2 (NT-CT) and rGRA6 to those predicted for endogenous GRA2 and GRA6 deleted of their putative signal peptide.

Protein	Number of aa	% Of α-helix[a]	% Of extended strand[a]	% Of random coil[a]
GRA2[b]	162	30.25	8.64	61.11
GRA6[c]	187	22.46	10.16	67.38
rGRA2	239	33.90	7.50	58.60
rGRA2 (NT-CT)	173	22.70	8.10	69.20
rGRA6	296	26.50	15.80	57.70

[a] https://npsa-prabi.ibcp.fr/cgi-bin/npsa_automat.pl?page=npsa_gor4.html.
[b] Amino acids 24 to 185 of GRA2 (RH).
[c] Amino acids 44 to 230 of GRA6 (RH).

Table 2
Comparison of the hydrophobicity criteria of the GRA2 AAHs (criteria definition for A and B in Refs. [23,24], respectively).

AAH	Number of aa	Net charge		Peak hydrophobic moment		Mean hydrophobicity	
		z		<μH> max		<H> (kcal/mol)	
		A	B	A	B	A	B
AAH1[a]	23	+3	+3	0.67	0.458	−0.22	0.237
AAH2[b]	16	+3	+3	0.41	0.271	−0.29	−0.053
AAH3[c]	21	+4	+4	0.45	0.201	−0.02	0.125
AAH1+2[d]	43	+6	+6	0.57	0.380	−0.20	0.177

[a] aa. 70 to 92.
[b] aa. 95 to 110.
[c] aa. 119 to 139.
[d] aa 70 to 112 [7].

the Hisx6 tags (Fig. 1), one can assume that the degradation takes place from each extremity of the recombinant protein. The major degradation products of 36 and 26 kDa would thus correspond to the trimming of 63 and 154 a.a., respectively.

A limitation encountered during our study was the spontaneous formation of big aggregates of the expressed recombinant proteins rGRA6 and rGRA2 (in a lesser extent) upon freezing. We have previously shown that the spontaneous formation of GRA protein aggregates is an intrinsic feature of the GRA proteins within the parasite and that this aggregation likely contributes to the formation of the dense granule storage organelles [18–20]. Yet, a fraction of soluble native GRA proteins, including soluble GRA2 and GRA6, is always recovered from the parasite dense granules as well as from the PV [4,13,21,22]. The recombinant protein aggregates observed in this study might thus reflect the natural dual behavior of the GRA proteins. Nevertheless, to eliminate the major aggregates, the recombinant proteins were systematically spun at 10,000 × g upon thawing and the experiments were performed on the supernatants, once their content in soluble proteins had been quantified.

GRA2 was previously shown to be the main initiator of MNN biogenesis [10], likely by deforming membrane vesicles present in the vacuolar space into membranous tubes by the use of its AAHs. Most of the proteins which sense membrane curvature through AAHs typically contain only one AAH, usually located in the N-terminal region. GRA2 is particular in the sense that it was predicted to contain either 3 AAHs (a.a. 70 to 92, 95 to 110 and 119 to 139, respectively) or alternatively, one long in-plane AAH1+2 (aa 70–112) followed by the AAH corresponding to aa 119 to 139 in its central region [7]. These AAHs (Supplementary Fig. 2), which all fit the Eisenberg criteria of hydrophobicity [23], were re-analyzed using the recently released Heliquest program (http://heliquest.ipmc.cnrs.fr/). Using the new criteria defined by Drin and Antonny [24], the GRA2 AAHs were also predicted as being able to remodel membranes (Table 2). The positioning of lysine residues at the AAH polar/apolar interfaces (Supplementary Fig. 2) would conveniently induce a snorkel effect. The long hydrocarbonated chains of lysine residues could indeed insert into the lipid acyl chains, thus favoring binding of the AAHs to membranes [25]. Furthermore, the three GRA2 AAHs display positive net charges (+3, +3 and +4, respectively) (Table 2), that are likely adapted to membranes enriched in negatively charged lipids. AAHs are described as being potentially unfolded in ionic buffer [26]. This does not seem to be the case for the GRA2 AAHs since CD analysis revealed a predominant α-helical pattern in rGRA2, when diluted in 20 mM MOPS, pH 7–500 mM NaCl (Fig. 2). Based on the quality and the intensity of the CD signal obtained for rGRA2 (Fig. 2), it is probable that both types of rGRA2 particles, the small ones (~10 nm in diameter) and the big ones (up to 40 nm in diameter) (Fig. 3B), whatever their state of association, would fold in α-helix. Together, these results emphasize the unusual properties of the GRA2 protein, which by an inplane AAH or by three AAHs, could sense and deform vesicles into membranous tubules. One could hypothesize that three AAHs might favor assembly of GRA2 monomers into big particles as long as the protein remains unbound to membranes and that the two first AAH then might associate to the vacuolar network membranes by forming an inplane long AAH (Supplementary Fig. 2).

Conflict of interest

None

Acknowledgments

The authors thank E. Gentilhomme (CRSSA, 38702, Grenoble, France) for help in electron microscopy, L. D. Sibley (Department of Molecular Microbiology, Washington University School of Medicine, Saint-Louis, MO), L. Pelosi and M.A. Hakimi (CNRS UMR 5163 – Joseph Fourier University, Grenoble 1) for sharing reagents. This work used the platform of the Grenoble Instruct Center (ISBG; UMS 3518 CNRS, CEA, UJF, EMBL) with support from FRISBI (ANR-10-INSB-05-02) and GRAL (ANR-10-LABX-49-01) within the Grenoble Partnership for Structural Biology and was supported by Région Rhône-Alpes (Grant from Cluster 10 on Infectious Diseases to CM). AB was the recipient of a PhD fellowship from the Rhône-Alpes Region and GE was supported by the Agence Nationale de la Recherche (ANR-08-BLAN-0271-CSD8 to WW and GS).

Appendix A. Supplementary data

Supplementary data related to this article can be found at http://dx.doi.org/10.1016/j.bbrc.2015.02.078.

References

[1] M. Lebrun, V.B. Carruthers, M.F. Cesbron-Delauw, Toxoplasma secretory proteins and their roles in cell invasion and intracellular survival, in: W.M. Weiss, K. Kim (Eds.), Toxoplasma Gondii: The Model Apicomplexan – Perspectives and Methods, second ed., Academic Press, London, 2013, pp. 390–455.
[2] C. Mercier, M.F. Delauw, Safe living within a parasitophorous vacuole: the recipe of success by Toxoplasma gondii, in: E. Ghigo (Ed.), Pathogen Interaction. At the Frontier of Cellular Microbiology, Transworld Res. Network, Kerala, India, 2012, pp. 1–18.
[3] C. Mercier, M.F. Cesbron-Delauw, Toxoplasma secretory granules: one population or more? Trends Parasitol. 31 (2015) 60–71.
[4] L.D. Sibley, I.R. Niesman, S.F. Parmley, et al., Regulated secretion of multilamellar vesicles leads to formation of a tubulo-vesicular network in host-cell vacuoles occupied by Toxoplasma gondii, J. Cell. Sci. 108 (1995) 1669–1677.
[5] C. Mercier, M.F. Cesbron-Delauw, L.D. Sibley, The amphipatic alpha-helices of the Toxoplasma protein GRA2 mediate post-secretory membrane association, J. Cell. Sci. 111 (1998a) 2171–2180.
[6] R.C. Magno, L. Lemgruber, R.C. Vommaro, et al., Intravacuolar network may act as a mechanical support for Toxoplasma gondii inside the parasitophorous vacuole, Microsc. Res. Tech. 67 (2005) 45–52.

[7] L. Travier, R. Mondragon, J.F. Dubremetz, et al., Functional domains of the Toxoplasma GRA2 protein in the formation of the membranous nanotubular network of the parasitophorous vacuole, Int. J. Parasitol. 38 (2008) 757–773.
[8] M.L. Reese, J.C. Boothroyd, A helical membrane-binding domain targets the Toxoplasma ROP2 family to the parasitophorous vacuole, Traffic 10 (2009) 1458–1470.
[9] C. Mercier, D.K. Howe, D.G. Mordue, et al., Targeted disruption of the GRA2 locus in Toxoplasma gondii decreases acute virulence in mice, Infect. Immun. 66 (1998b) 4176–4182.
[10] C. Mercier, J.F. Dubremetz, B. Rauscher, et al., Biogenesis of nanotubular network in Toxoplasma parasitophorous vacuole induced by parasite proteins, Mol. Biol. Cell. 13 (2002) 2397–2409.
[11] H. Charif, F. Darcy, G. Torpier, et al., Toxoplasma gondii: characterization and localization of antigens secreted from tachyzoites, Exp. Parasitol. 71 (1990) 114–124.
[12] M.F. Cesbron-Delauw, C. Boutillon, C. Mercier, et al., Amino acid sequence requirements for the epitope recognized by a monoclonal antibody reacting with the secreted antigen GP28.5 of Toxoplasma gondii, Mol. Immunol. 29 (1992) 1375–1382.
[13] E. Labruyère, M. Lingnau, C. Mercier, et al., Differential membrane targeting of the secretory proteins GRA4 and GRA6 within the parasitophorous vacuole formed by Toxoplasma gondii, Mol. Biochem. Parasitol. 102 (1999) 311–324.
[14] M. Golkar, M.A. Shokrgozar, S. Rafati, et al., Evaluation of protective effect of recombinant dense granule antigens GRA2 and GRA6 formulated in monophosphoryl lipid A (MPL) adjuvant against Toxoplasma chronic infection in mice, Vaccine 25 (2007) 4301–4311.
[15] S. Dabrowski, J. Kur, Cloning, over-expression, and purification of the recombinant His-tagged SSB protein of Escherichia coli and use in polymerase chain reaction amplification, Protein. Expr. Purif. 16 (1999) 96–102.
[16] J. Garnier, J.F. Gibrat, B. Robson, GOR method for predicting protein secondary structure from amino acid sequence, Methods Enzymol. 266 (1996) 540–553.
[17] C. Gendrin, A. Bittame, C. Mercier, et al., Post-translational membrane sorting of the Toxoplasma gondii GRA6 protein into the parasite-containing vacuole is driven by its N-terminal domain, Int. J. Parsitol. 40 (2010) 1325–1334.
[18] L. Braun, L. Travier, S. Kieffer, et al., Purification of Toxoplasma dense granule proteins reveals that they are in complexes throughout the secretory pathway, Mol. Biochem. Parasitol. 157 (2008) 13–21.
[19] C. Gendrin, C. Mercier, L. Braun, et al., Toxoplasma gondii uses unusual sorting mechanisms to deliver transmembrane proteins into the host-cell vacuole, Traffic 9 (2008) 1665–1680.
[20] M.F. Cesbron-Delauw, C. Gendrin, L. Travier, et al., Apicomplexa in mammalian cells: trafficking to the parasitophorous vacuole, Traffic 9 (2008) 657–664.
[21] L. Lecordier, C. Mercier, L.D. Sibley, et al., Transmembrane insertion of the Toxoplasma gondii GRA5 protein occurs after soluble secretion into the host cell, Mol. Biol. Cell. 10 (1999) 1277–1287.
[22] K.D. Adjogble, C. Mercier, J.F. Dubremetz, et al., GRA9, a new Toxoplasma gondii dense granule protein associated with the intravacuolar network of tubular membranes, Int. J. Parasitol. 34 (2004) 1255–1264.
[23] D. Eisenberg, R.M. Weiss, T.C. Terwilliger, The helical hydrophobic moment: a measure of the amphiphilicity of a helix, Nature 299 (1982) 371–374.
[24] G. Drin, B. Antonny, Amphipathic helices and membrane curvature, FEBS Lett. 584 (2010) 1840–1847.
[25] M. Monné, I. Nilsson, M. Johansson, et al., Positively and negatively charged residues have different effects on the position in the membrane of a model transmembrane helix, J. Mol. Biol. 284 (1998) 1177–1183.
[26] J.L. Gallop, C.C. Jao, H.M. Kent, P.J. Butler, et al., Mechanism of endophilin N-BAR domain-mediated membrane curvature, EMBO J. 25 (2006) 2898–2910.